Electronic Supplementary Information

Ligand exchange in quaternary alloyed nanocrystals – a spectroscopic study

Grzegorz Gabka[a], Piotr Bujak[a*], Kamila Giedyk[a], Kamil Kotwica[a], Andrzej Ostrowski[a], Karolina Malinowska[b], Wojciech Lisowski[c], Janusz W. Sobczak[c] and Adam Pron[a]

[a]Faculty of Chemistry, Warsaw University of Technology Noakowskiego 3, 00-664 Warsaw, Poland

[b]Faculty of Chemistry, University of Warsaw, Pasteura 1, 02-093 Warsaw, Poland

[c]Institute of Physical Chemistry, Polish Academy of Science, Kasprzaka 44/52, 01-224 Warsaw, Poland

Corresponding Author

*E-mail: piotrbujakchem@poczta.onet.pl

Experimental

Synthesis of copper(II) oleate[1]

Copper(II) oleate was prepared by reacting $CuCl_2$ with sodium oleate. Sodium oleate (80 mmol, 29.7 g) and $CuCl_2 \times 2H_2O$ (40 mmol, 6.9 g) were dissolved in a mixed solvent composed of 80 mL of ethanol, 60 mL of water and 140 mL of hexane. The mixture was heated to 70 °C and then kept at this temperature for four hours. The organic layer containing the desired product was washed three times with 30 mL of water in a separatory funnel. After washing, hexane layer was evaporated and the resulting product (copper(II) oleate) was recovered in a form of a green waxy solid.

Characterization of Cu-In-Zn-S nanocrystals

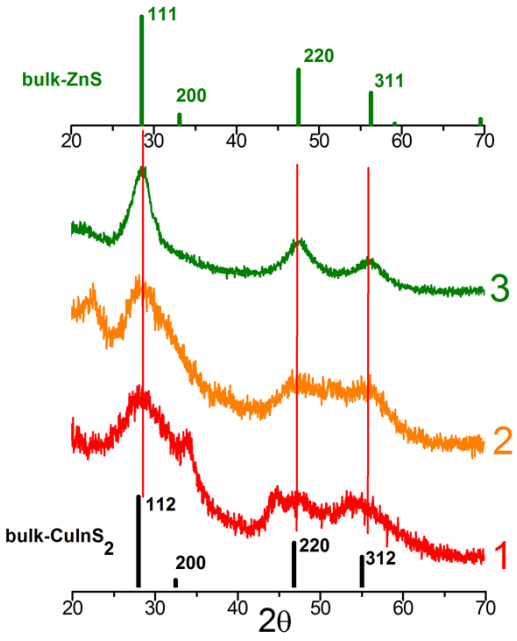

Figure S1. X-ray diffractogram of alloyed Cu-In-Zn-S quaternary nanocrystals obtained from reaction mixtures of Cu/In/Zn/DDT ratio = 1/13/20/21 (batch 1); 1/13/25/50 (batch 2) and 1/38/56/116 (batch 3). For comparison purposes, XRD patterns of the cubic[2] ZnS crystal (top patterns) and the roquesite[3] $CuInS_2$ crystal (bottom patterns) are also provided.

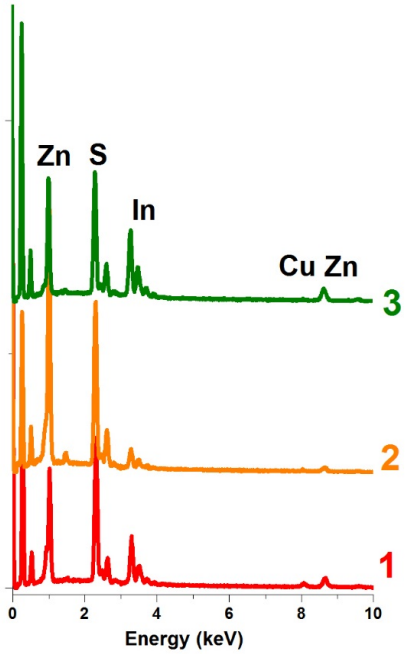

Figure S2. Energy-dispersive spectra of Cu-In-Zn-S nanocrystals.

Table S1. EDS characteristics of alloyed Cu-In-Zn-S nanocrystals.

	Cu/In/Zn/DDT[a]	Cu/In/Zn[b]
1	**1/13/10/21**	**1.0/2.1/3.9**
2	**1/13/25/50**	**1.0/2.7/15.6**
3	**1/38/56/116**	**1.0/15.0/24.0**

[a]precursors molar ratio; [b]ratio of elements in the nanocrystals from EDS

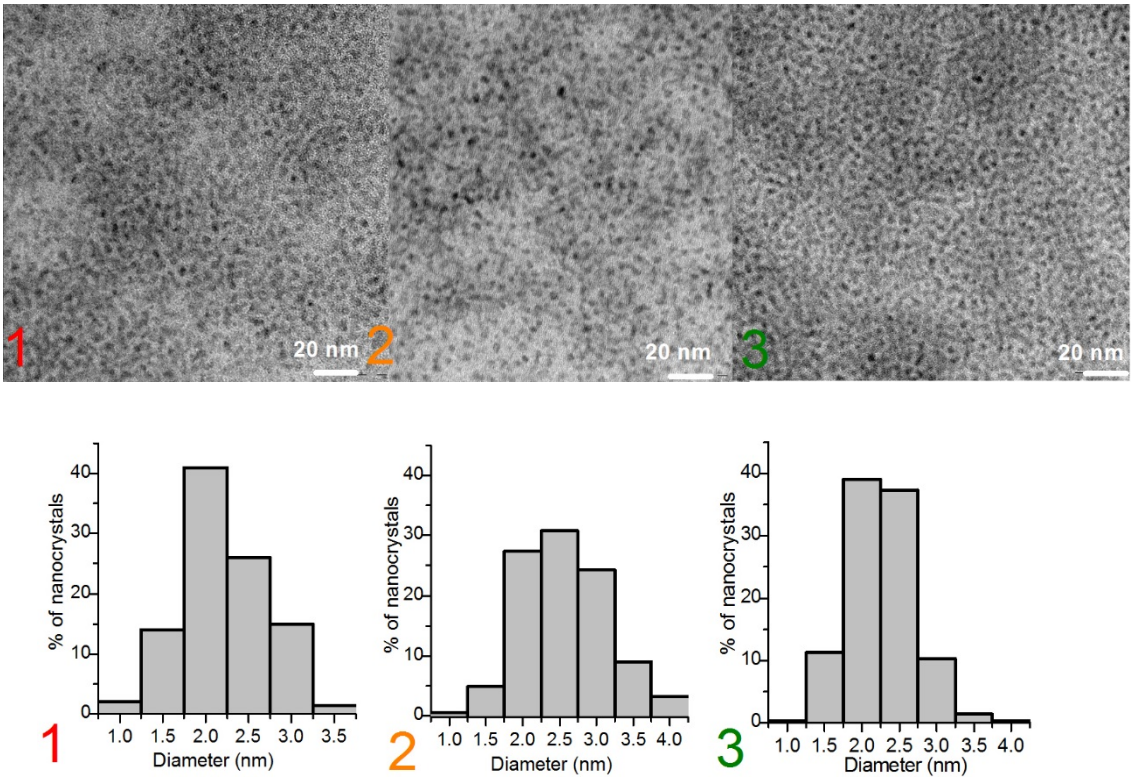

Figure S3. TEM images and histograms of Cu-In-Zn-S nanocrystals.

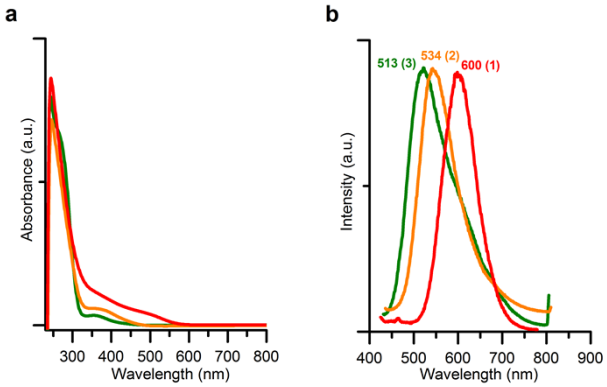

Figure S4. Absorption (a) and emission spectra of the Cu-In-Zn-S nanocrystals

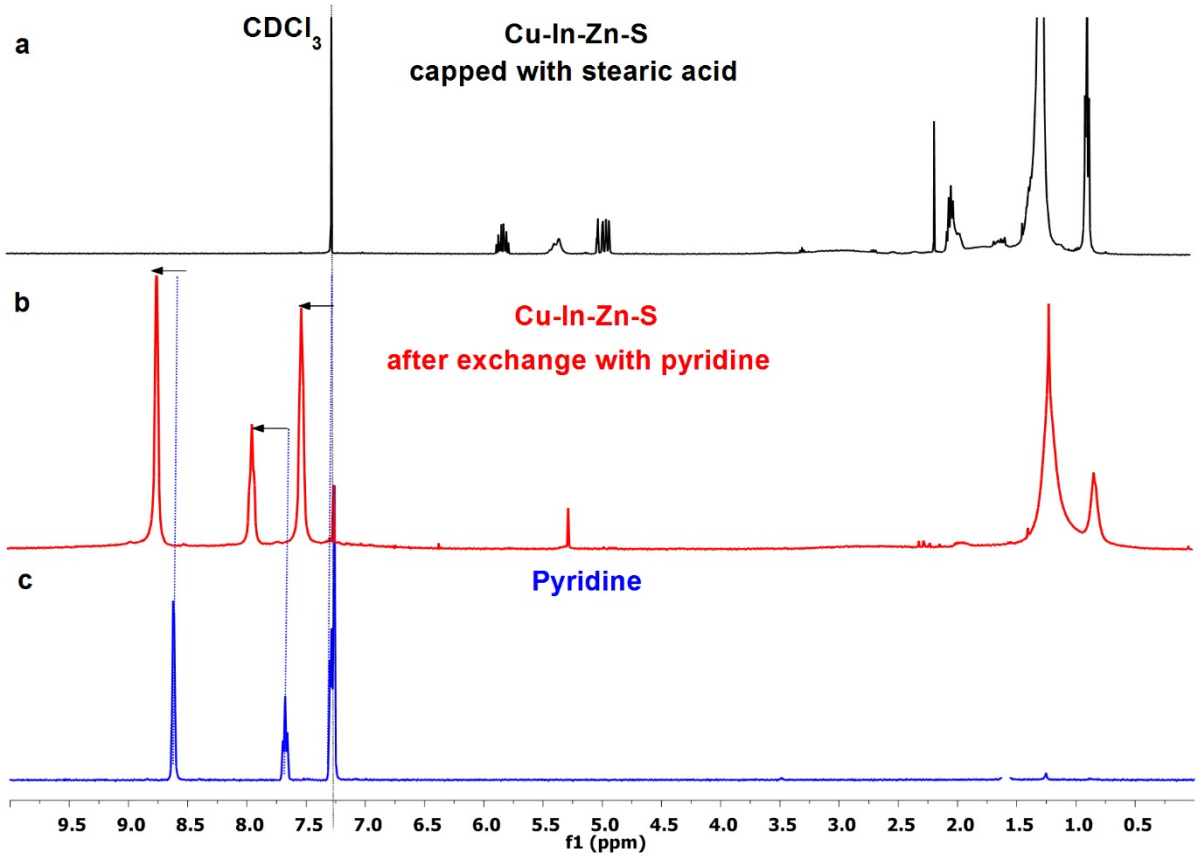

Figure S5. ^{1}H NMR spectra of stearic acid – capped Cu-In-Zn-S nanocrystals before (a) and after (b) exchange with pyridine and of pyridine (c) in $CDCl_3$.

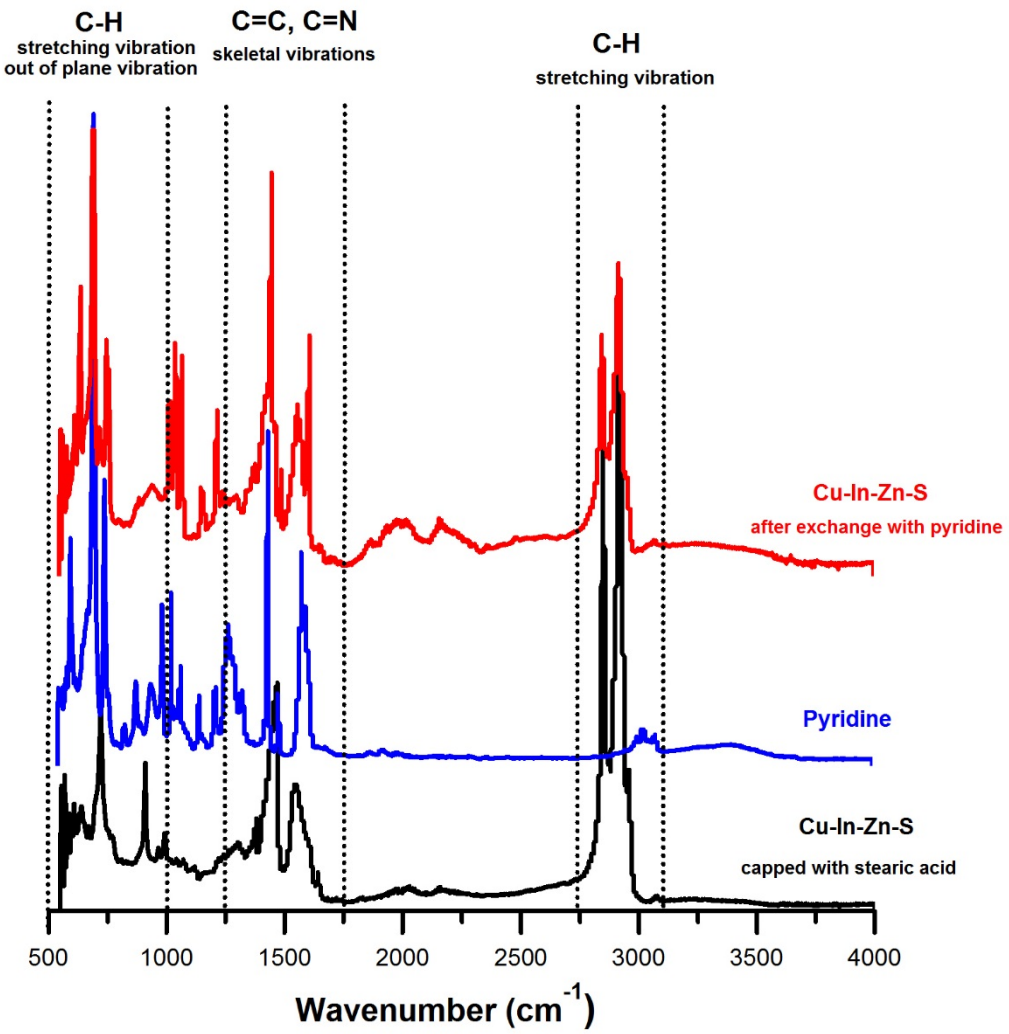

Figure S6. FT-IR spectra of pyridine and of Cu-In-Zn-S nanocrystals before and after exchange with pyridine.

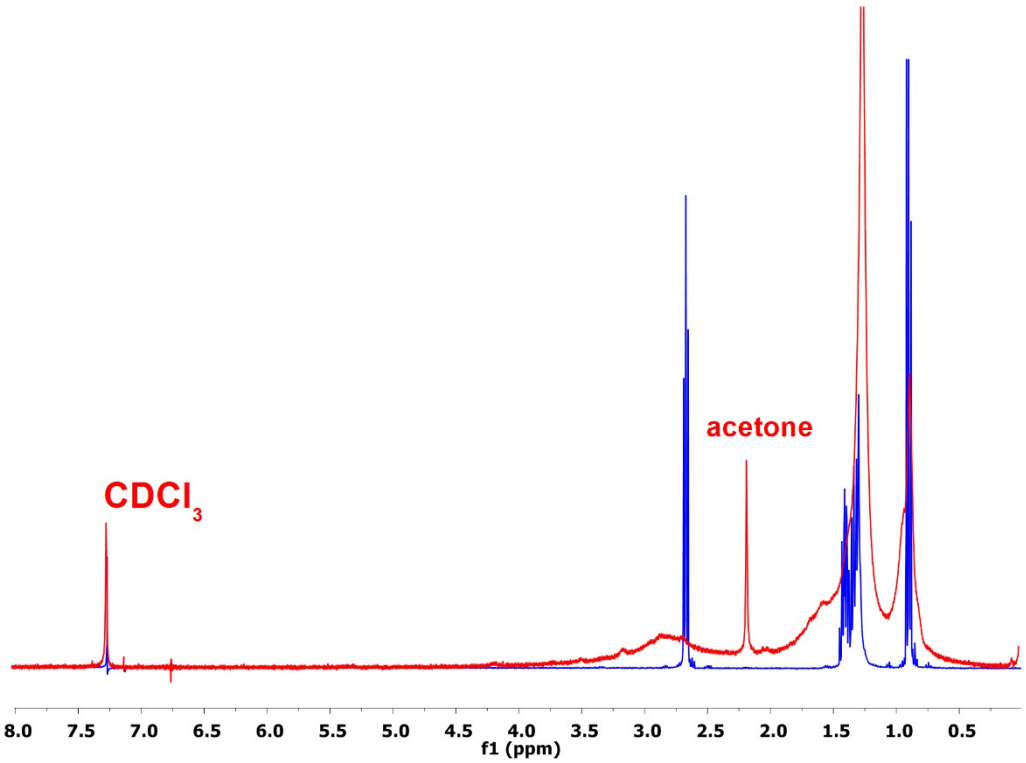

Figure S7. ^{1}H NMR spectra of n-butylamine (blue) and of pyridine-capped Cu-In-Zn-S nanocrystals after ligand exchange with this compound (red) in $CDCl_3$.

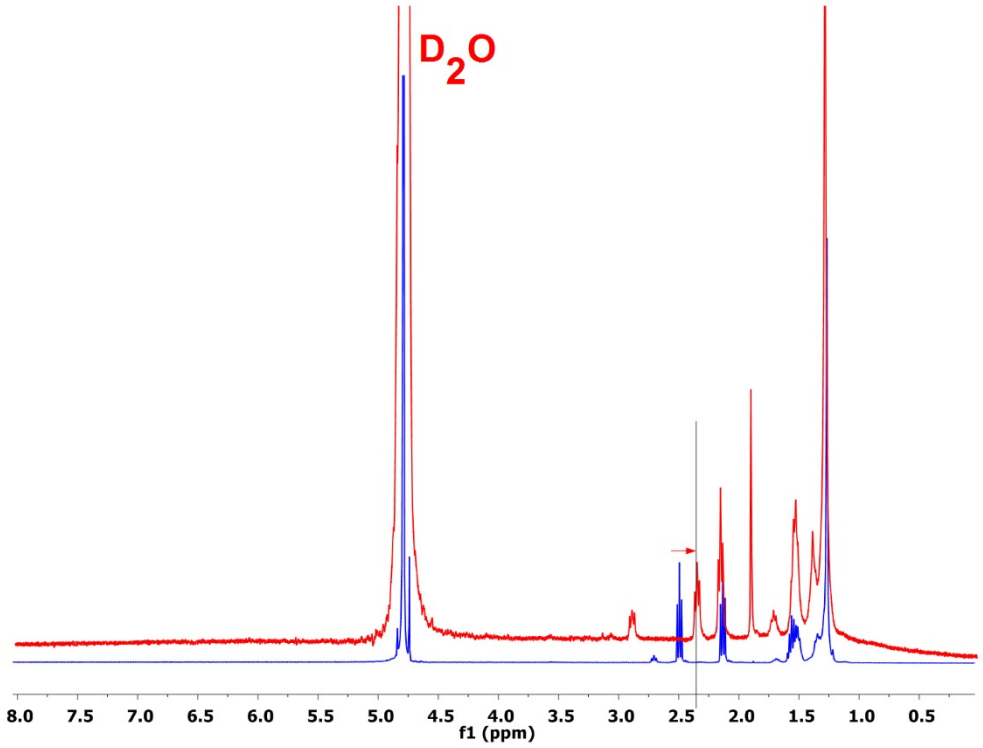

Figure S8. ^{1}H NMR spectra of 11-mercaptoundecanoic acid (blue) and of pyridine-capped Cu-In-Zn-S nanocrystals after ligand exchange with this compound (red) in D_2O (pH = 9.0).

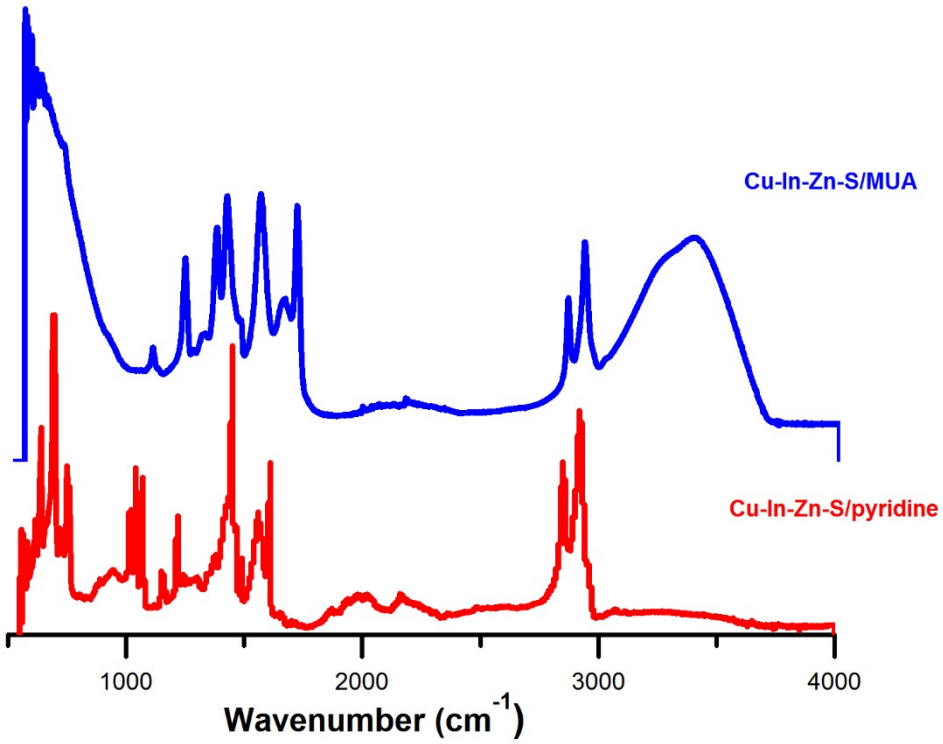

Figure S9. FT-IR spectra of pyridine-capped Cu-In-Zn-S nanocrystals and of 11-mercaptoundecanoic acid-capped Cu-In-Zn-S nanocrystals.

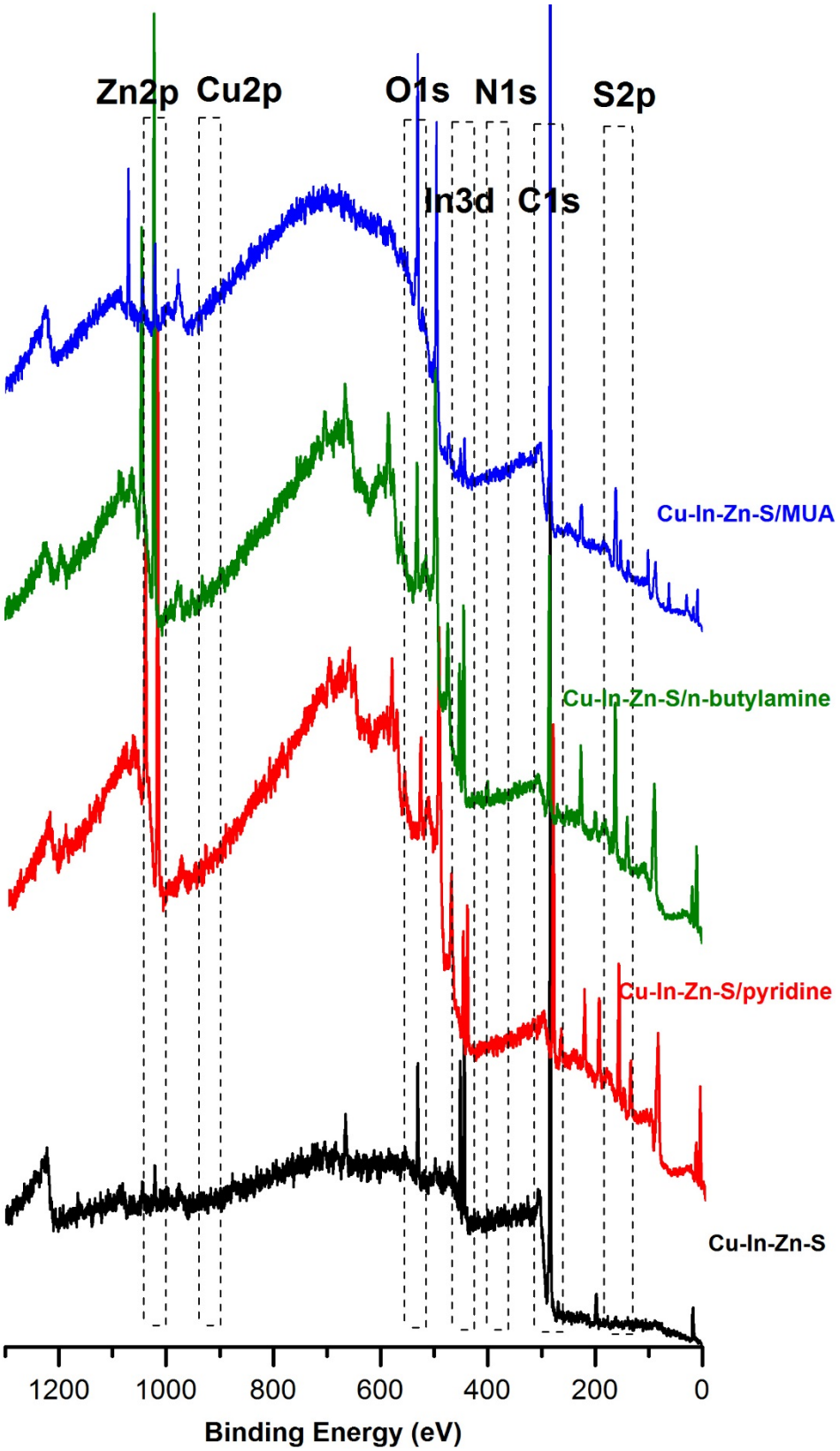

Figure S10. XPS survey spectra of stearic acid – capped Cu-In-Zn-S nanocrystals (black), pyridine – capped Cu-In-Zn-S nanocrystals (red), n-butylamine – capped Cu-In-Zn-S nanocrystals (green), MUA – capped Cu-In-Zn-S nanocrystals (blue).

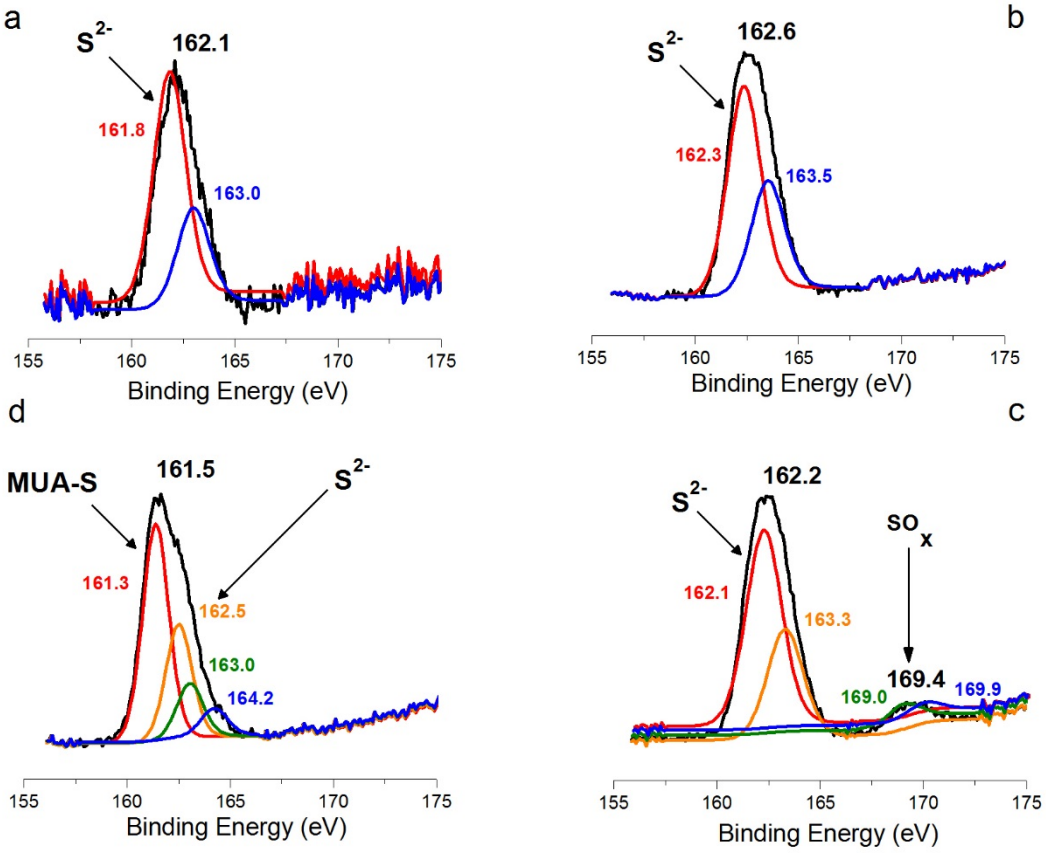

Figure S11. The high-resolution S2p XPS spectra of (a) stearic acid-, (b) pyridine-, (c) n-butylamine-, (d) MUA-capped Cu-In-Zn-S nanocrystals. Black lines-original spectra, color lines-deconvoluted spectra.

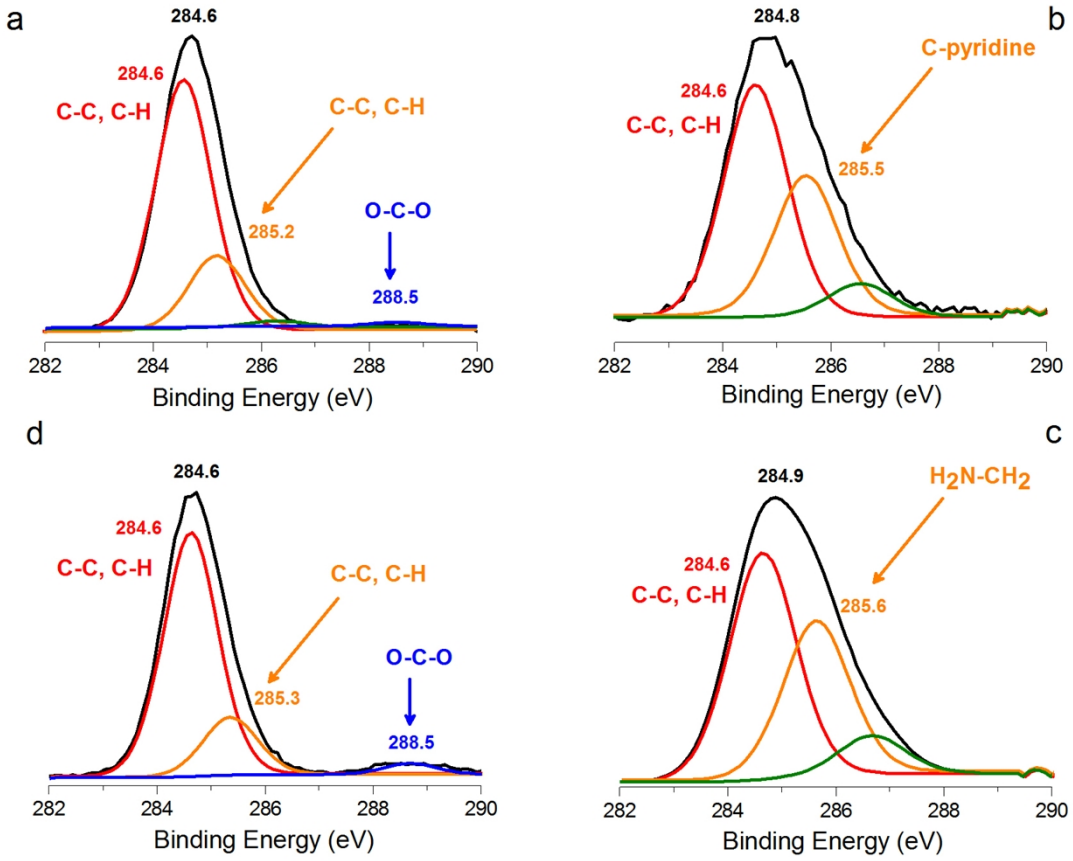

Figure S12. The high-resolution C1s XPS spectra of (a) stearic acid-, (b) pyridine-, (c) n-butylamine-, (d) MUA-capped Cu-In-Zn-S nanocrystals. Black lines – original spectra, color lines-deconvoluted spectra.

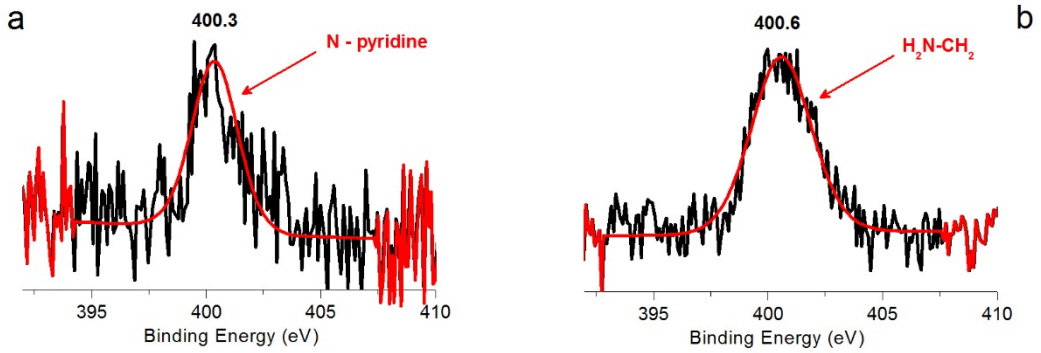

Figure S13. The high-resolution N1s XPS spectra of (a) pyridine-, (b) n-butylamine-capped Cu-In-Zn-S nanocrystals. Black lines-original spectra, red lines-deconvoluted spectra.

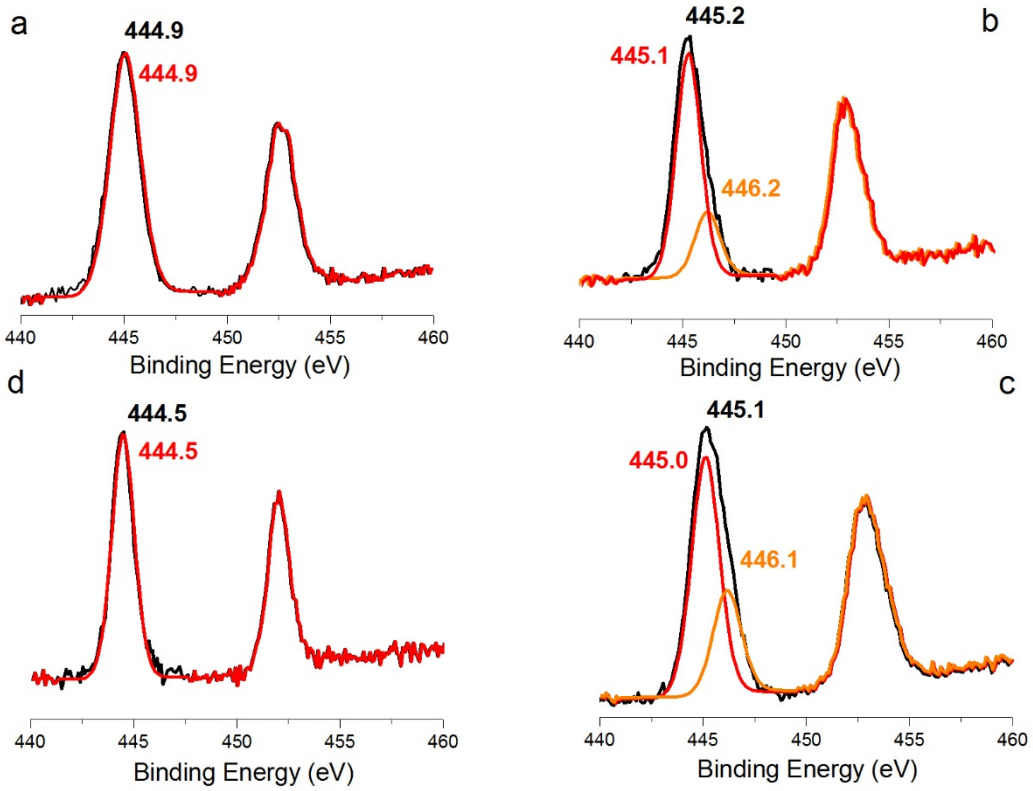

Figure S14. The high-resolution In3d XPS spectra of (a) stearic acid-, (b) pyridine-, (c) n-butylamine-, (d) MUA-capped Cu-In-Zn-S nanocrystals. Black lines-original spectra, color lines-deconvoluted spectra.

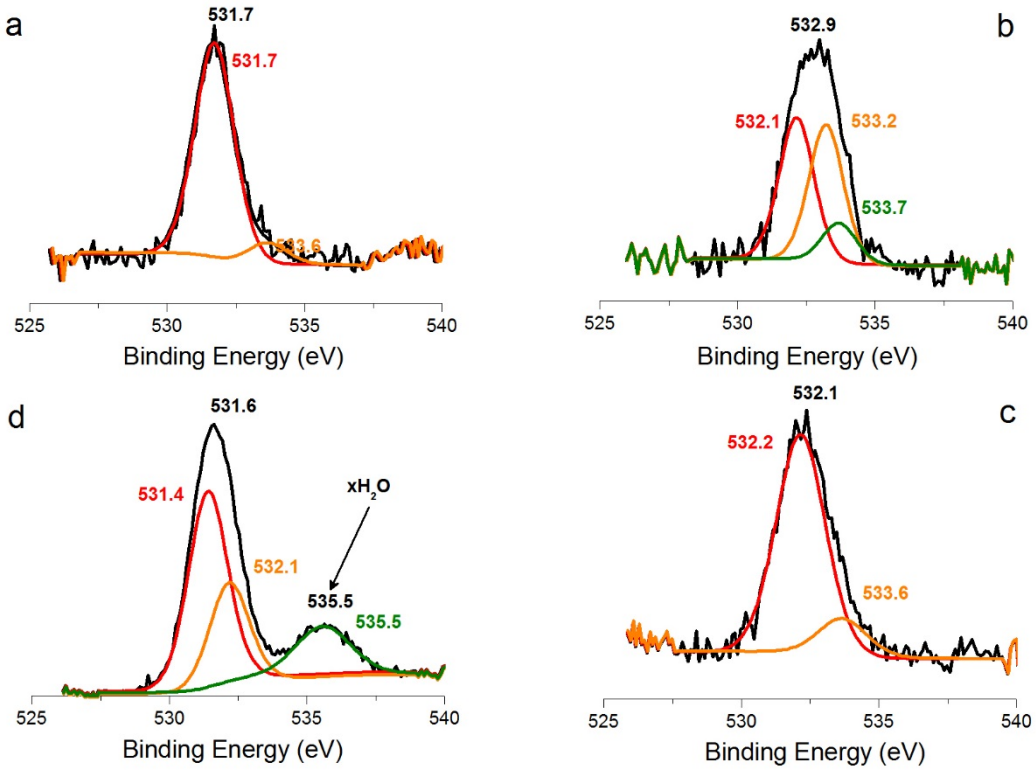

Figure S15. The high-resolution O1s XPS spectra of (a) stearic acid-, (b) pyridine-, (c) n-butylamine-, (d) MUA-capped Cu-In-Zn-S nanocrystals. Black lines-original spectra, color lines-deconvoluted spectra.

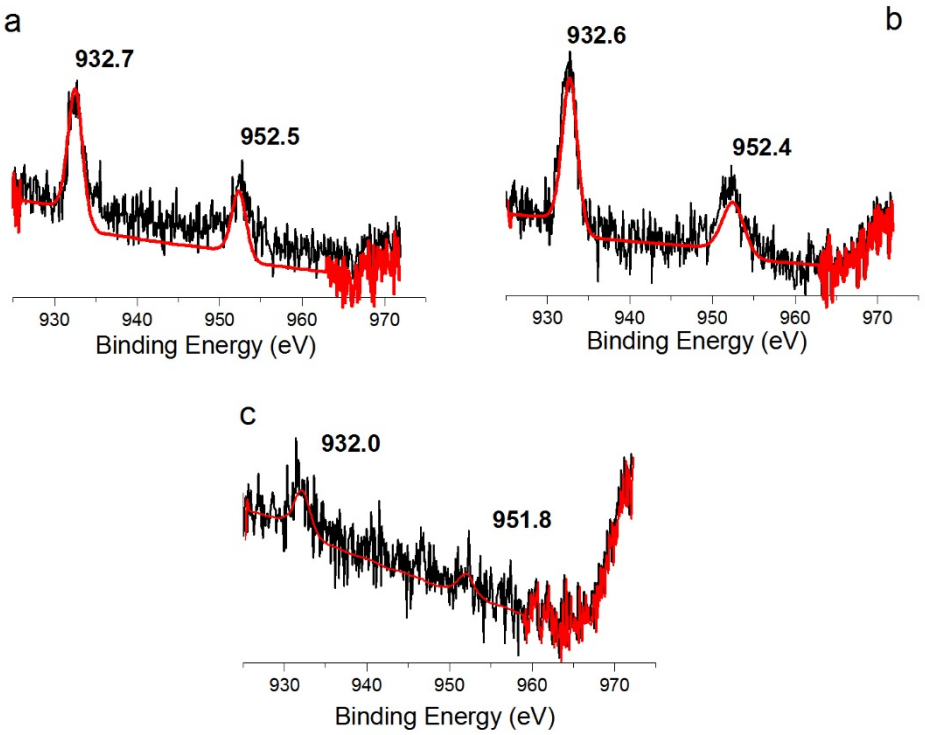

Figure S16. The high-resolution Cu2p XPS spectra of (a) pyridine-, (b) n-butylamine-, (c) MUA-capped Cu-In-Zn-S nanocrystals. Black lines-original spectra, red lines-deconvoluted spectra.

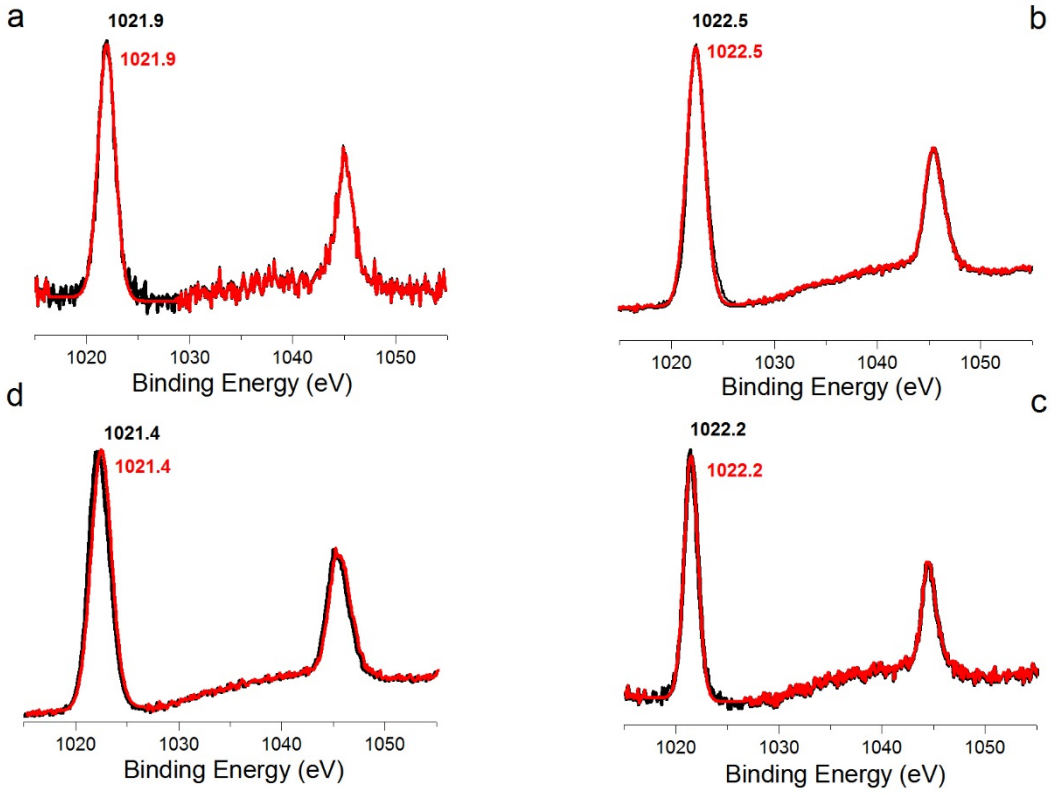

Figure S17. The high-resolution Zn2p XPS spectra of (a) pyridine-, (b) n-butylamine-, (c) MUA-capped Cu-In-Zn-S nanocrystals. Black color-original spectra, red color-deconvoluted spectra.

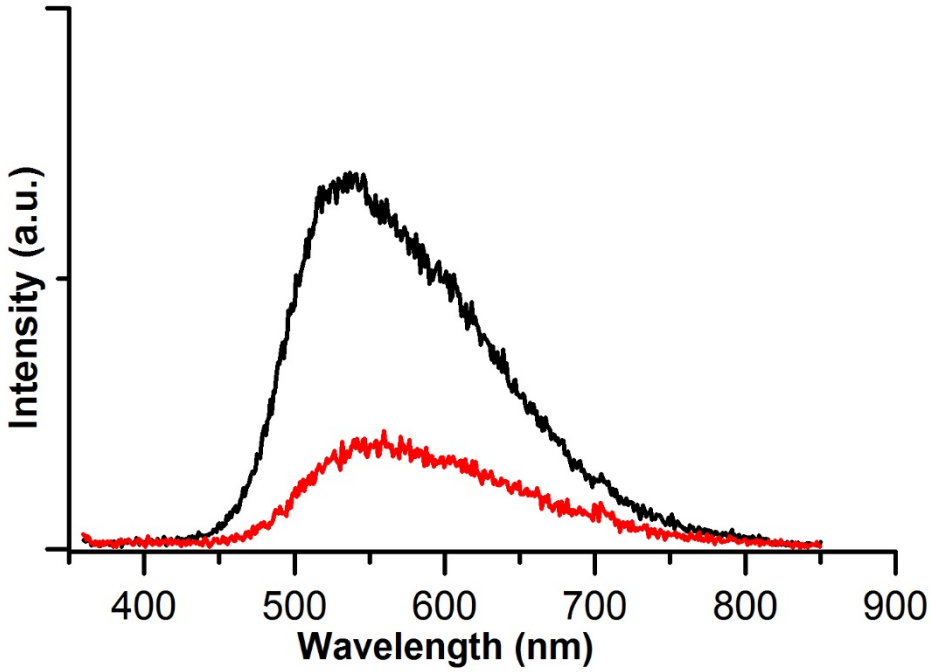

Figure S18. Emission spectra of (black) stearic acid, (red) pyridine – capped Cu-In-Zn-S nanocrystals in chloroform.

Characterization of Cu-In-S nanocrystals

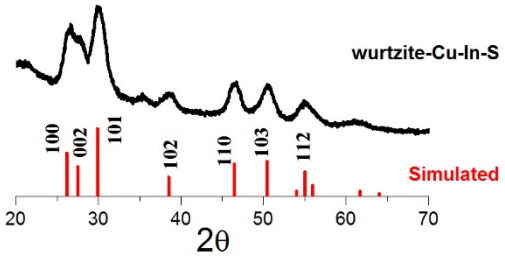

Figure S19. Experimental and simulated[4] XRD patterns of Cu-In-S nanocrystals with a wurtzite structure.

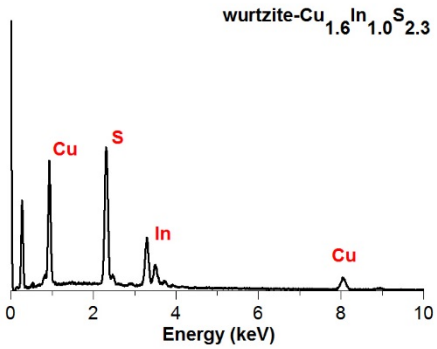

Figure S20. Energy dispersive spectrum of wurtzite $Cu_{1.6}In_{1.0}S_{2.3}$ nanocrystals.

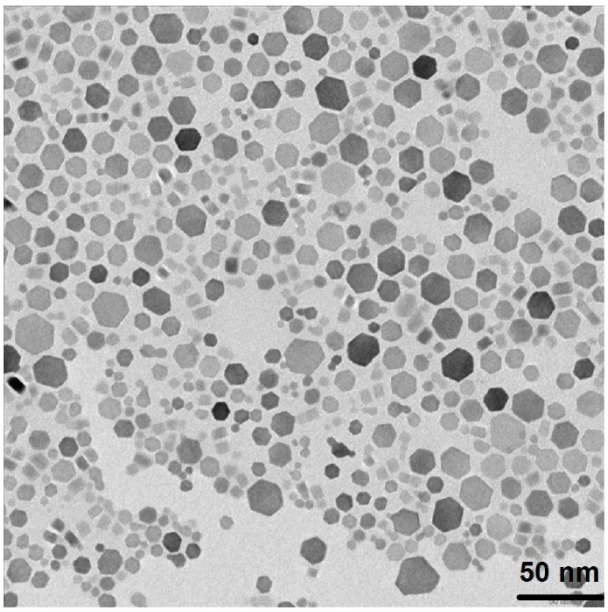

Figure S21. TEM image of wurtzite $Cu_{1.6}In_{1.0}S_{2.3}$ nanocrystals.

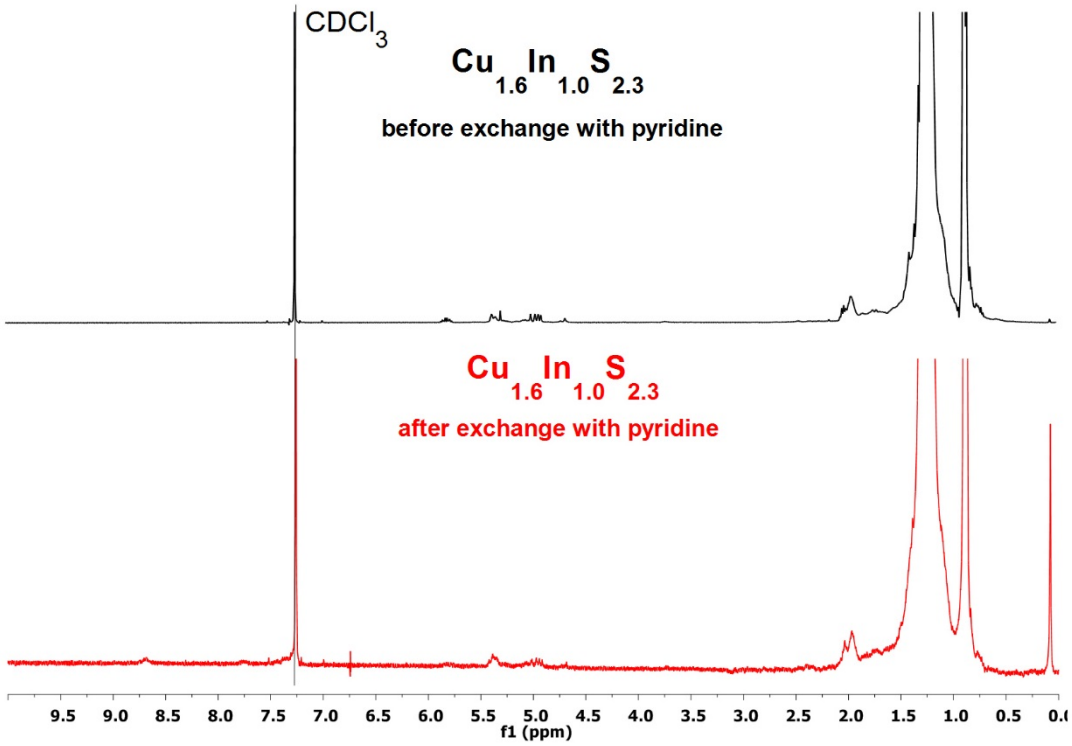

Figure S22. ^{1}H NMR spectra of $Cu_{1.6}In_{1.0}S_{2.3}$ nanocrystals before and after exchange with pyridine in $CDCl_3$.

Characterization of Ag-In-Zn-S alloyed nanocrystals

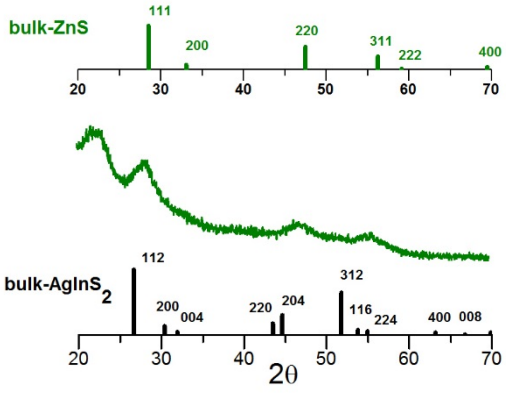

Figure S23. X-ray diffractogram of alloyed Ag-In-Zn-S quaternary nanocrystals obtained from reaction mixtures of Ag/In/Zn/DDT ratio = 1/5/14/26. For comparison purposes, XRD patterns of the cubic[2] ZnS crystal (top patterns) and the tetragonal[5] $AgInS_2$ crystal (bottom patterns) are also provided.

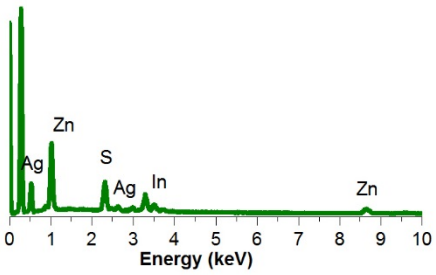

Figure S24. Energy dispersive spectrum of alloyed Ag-In-Zn-S nanocrystals. (Ag/In/Zn = 1.0/3.9/12.1)

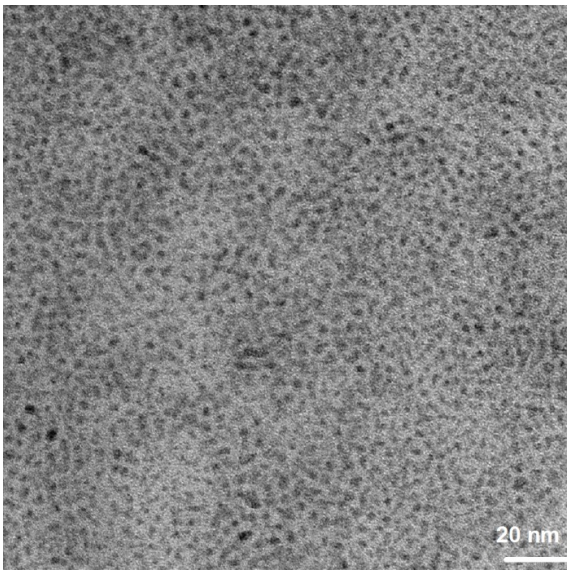

Figure S25. TEM image of alloyed Ag-In-Zn-S nanocrystals.

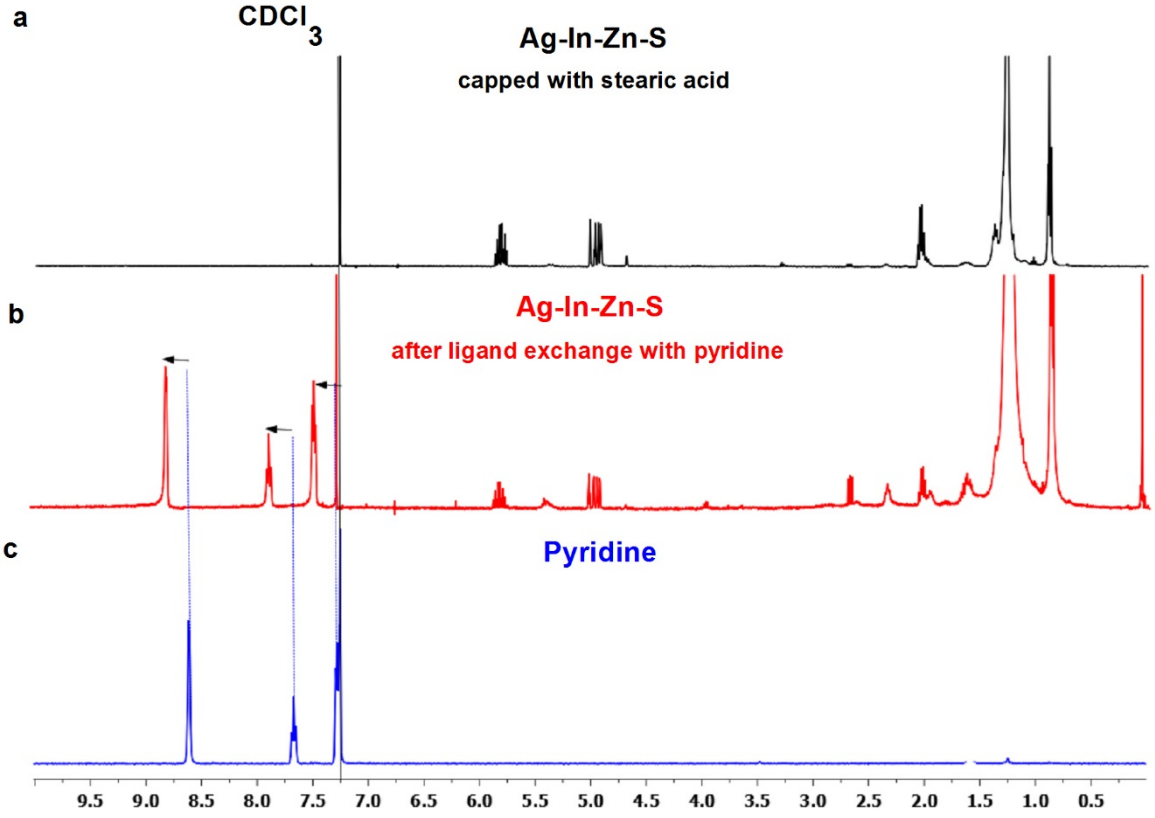

Figure S26. ^{1}H NMR spectra of stearic acid – capped Ag-In-Zn-S nanocrystals before (a) and after (b) exchange with pyridine and of pyridine (c) in $CDCl_3$.

References:

(1) J. Park, K. An, Y. Hwang, J.-G. Park, H.-J. Noh, J.-Y. Kim, J.-H. Park, N.-M. Hwang, T. Heyon, *Nat. Materials,* 2004, **3**, 891-895.

(2) Powder Diffraction File, No. 50566; The JCPD International Centre for Diffraction Data: Swarthmore, PA, 1990.

(3) Powder Diffraction File, No. 471372; The JCPD International Centre for Diffraction Data: Swarthmore, PA, 1990.

(4) J. Chang and E. R. Waclawik, *CrystEngComm*, 2013, **15**, 5612-5619.

(5) Powder Diffraction File, No. 251330; The JCPD International Centre for Diffraction Data: Swarthmore, PA, 1990.